Open Quantum Dynamics Theory for Coulomb Potentials: Hierarchical Equations of Motion for Atomic Orbitals (AO-HEOM)

Yankai Zhang and Yoshitaka Tanimura[a)]
Department of Chemistry, Graduate School of Science, Kyoto University, Kyoto 606-8502, Japan

(Dated: Last updated: 28 August 2025)

We investigate the quantum dynamics of Coulomb potential systems in thermal environments. We study these systems within the framework of open quantum dynamics theory, focusing on preserving the rotational symmetry of the entire system, including the heat bath. Thus, we employ a three-dimensional rotationally invariant system-bath (3D-RISB) model to derive reduced hierarchical equations of motion for atomic orbitals (AO-HEOM) that enable a non-perturbative and non-Markovian treatment of system-bath interactions at finite temperatures in a numerically rigorous manner. The result was examined by calculating the linear absorption spectrum of a system coupled to isotropic thermal environments.

I. INTRODUCTION

Coulomb potentials encompass a wide variety of physical systems characterized by interactions among charged particles.[1–5] The potential is conventionally represented as proportional to $\propto 1/r$, where r denotes the radial distance from the center of charge, while a short-range correction term $\propto e^{-r/\rho}/r^n$ is often included, where n is an integer and ρ is the characteristic screening length. Hydrogen atoms are a well-known example, but the same potential has been employed to describe problems in condensed phases, such as the color center problem in ionic crystals[6–8] and interactions between ions in ionic solvents.[3,4]

Recent advances in CPU power and algorithmic development have enabled the efficient dynamic simulation of isolated Coulomb systems, despite the persistence of certain mathematical challenges.[9] In contrast, simulating quantum dynamics under the influence of thermal environments (baths) remains a significant challenge. This difficulty has been circumvented in the case of vacuum radiation fields as a bath, where thermal excitations are absent. Indeed, such scenarios represent one of the earliest applications of open quantum systems theory. In such cases, the system-bath (S-B) coupling is weak, and the quantum effects of thermal fluctuations are negligible due to the much larger excitation energy compared to the thermal energy. Under these conditions, several assumptions become valid, including the rotating wave approximation, the factorized initial condition, and the Markovian approximation. These allow the qualitative influence of the bath to be incorporated into the dynamics of the system's energy eigenstates, with relaxation processes characterized by transition rates, typically expressed in terms of Einstein coefficients.[10,11]

In condensed phases, where thermal excitations play a crucial role, a non-Markovian treatment of fluctuation, which is a consequence of the quantum fluctuation-dissipation theorem, is significant.[12–15] Over the past three decades, it has been recognized that applying the Markov approximation to spin-boson systems under thermal conditions leads to unphysical anomalies, such as equal populations of ground and excited states irrespective of temperature.[16–20] These inconsistencies can be resolved using the hierarchical equations of motion (HEOM)[12–15] and the quasi-adiabatic path-integral (QUAPI) approach,[21–23] both of which are non-perturbative and non-Markovian frameworks that rigorously and quantitatively account for the influence of thermal environments. However, a more fundamental question remains: What is the appropriate characterization of heat baths that interact with Coulombic systems exhibiting rotational symmetry?

To gain deeper insight into this issue, we introduce the rotationally invariant system-bath (RISB) model, originally developed by Gefen, Ben-Jacob, and Caldeira to study current-biased tunnel junctions under dissipative environments.[24] The RISB framework has since been applied to explore quantum dynamics in two-dimensional (2D) rotors,[25] Aharonov–Bohm rings,[26] and three-dimensional (3D) rotors.[27;28] The present study extends the RISB model to examine the dynamics of systems with atomic orbits that exhibit rotational symmetry. As an application, we consider a hydrogen atom coupled to a thermal environment modeled by the 3D-RISB. Because quantum entanglement between the system and the bath plays a critical role in determining the dynamics, we use the Hierarchical Equations of Motion for Atomic Orbitals (AO-HEOM) approach, which is numerically "exact". To validate our theoretical framework, we compute the linear response spectrum of the Coulomb system across a range of bath temperatures and coupling strengths.

This paper is organized as follows. In Sec. II, we describe the 3D-RISB model for a Coulomb potential system. The AO-HEOM for 3D-RISB are then presented. A numerical demonstration is given in Sec. III. Section IV is devoted to concluding remarks.

[a)]Author to whom correspondence should be addressed: tanimura.yoshitaka.5w@kyoto-u.jp

II. HEOM FOR COULOMB POTENTIAL SYSTEM

A. The 3D-RISB model

It is crucial to emphasize that although the Ohmic SDF has been assumed for the study of Markovian dynamics in the spin–boson systems, this model exhibits anomalous dynamical behavior (an infrared anomaly) at finite temperatures.[16–20] This arises because quantum thermal noise is inherently non-Markovian in nature because its correlation time and amplitude must satisfy the uncertainty principle.[19,20] Even if S-B interactions are weak, there are multiple interactions between the system and the bath during the noise correlation time in non-Markovian cases, requiring a non-perturbative treatment. Consequently, the system and the bath become entangled, resulting in system dynamics that differ significantly from those described under the factorized assumption. For example, while the Liouvillian of classical and quantum harmonic systems has the same form, but only the quantum system entangled with a heat bath incorporates $\hbar$ in its thermal equilibrium distribution.[29]

Accordingly, systems exhibiting rotational symmetry are expected to possess periodic entanglement. Consequently, the total system–including the bath–must preserve rotational symmetry. To accommodate this requirement, 2D- and 3D-RISB models have been developed.[25,27] In the classical limit, these models converge to the classical Brownian rotor system, thereby providing a unified framework that seamlessly bridges quantum and classical regimes. It is important to note that if the heat bath fails to preserve the same rotational symmetry as the primary system, the resulting dynamics deviate significantly from expected behavior. For instance, when a quantum rotor is analyzed using the conventional Caldeira—Leggett (CL) model, the characteristic discretized rotational band structure fails to emerge.[30]

The 3D-RISB model is expressed in a Cartesian coordinate system as

$$\hat{H}_{tot} = \hat{H}_S + \sum_{\alpha=x,y,z} \hat{H}^\alpha_{I+B}, \tag{1}$$

where the primary system involved the Coulomb potential, which is defined by

$$\hat{H}_S = \sum_{\alpha=x,y,z} \frac{\hat{p}^2_\alpha}{2M} - \frac{A}{r}, \tag{2}$$

where $\hat{p}_\alpha$ is the momentum operator in the $\alpha = x, y,$ and z direction and M is the mass of the system. The Coulomb potential is expressed in terms of the radius from the center of charge, denoted by $r \equiv \sqrt{x^2 + y^2 + z^2}$ and the constant to describe the excitation energy A. The primary system is independently coupled to three heat baths in the x, y, and z directions (3D baths) expressed as[25–28]

$$\hat{H}^\alpha_{I+B} = \sum_j \left\{ \frac{(\hat{p}^\alpha_j)^2}{2m^\alpha_j} + \frac{1}{2} m^\alpha_j (\omega^\alpha_j)^2 \left(\hat{q}^\alpha_j - \frac{c^\alpha_j \hat{V}_\alpha}{m^\alpha_j (\omega^\alpha_j)^2} \right)^2 \right\}, \tag{3}$$

where m^α_j, $\hat{p}^\alpha_j$, $\hat{q}^\alpha_j$ and ω^α_j represent the mass, momentum, coordinate, and frequency, respectively, of the jth bath oscillator mode in the α direction.

We can regard these baths as arising from the local environments due to the surrounding atoms or molecules. The system part of the system-bath interactions is, for example, defined as $(\hat{V}_x, \hat{V}_y, \hat{V}_z) \equiv (\hat{x}, \hat{y}, \hat{z})$, and c^α_k is the system-bath coupling constant. We include the counter terms that are introduced to maintain the translational symmetry of the system Hamiltonian.[31] The harmonic bath in the α direction is characterized by the spectral distribution function, defined as $J^\alpha(\omega) = \sum_k [\hbar (c^\alpha_k)^2 / 2m^\alpha_k \omega^\alpha_k] \delta(\omega - \omega^\alpha_k)$, and the inverse temperature, $\beta \equiv 1/k_B T$, where k_B is the Boltzmann constant.

To adapt the HEOM formalism, we use the Drude spectral density expressed as[14,15]

$$J^\alpha(\omega) = \frac{\hbar \eta_\alpha}{\pi} \frac{\gamma^2_\alpha \omega}{\gamma^2_\alpha + \omega^2}, \tag{4}$$

where $\alpha = x, y,$ and z. It should be noted that $J^\alpha(\omega)$ does not have to be identical for different α directions. In particular, they will differ when the surrounding environment is anisotropic. Such a situation can also be achieved by applying a Stark electric field in a specific direction.[27] If necessary, we can also set anisotropic environments, for example, in the xy direction by correlating the bath modes in the $\alpha = x$ and y direction.[32]

B. AO-HEOM

The method we use to solve the dynamics of the reduced density operator is the HEOM, which provides a non-Markovian approach to numerically accurately solve even in the strong S-B interaction case.[12–15] The hierarchical structure was introduced to describe the entanglement that arises from multiple interactions with the heat bath.[14,15] In this paper, we adopt the $[K_\alpha - 1/K_\alpha]$ Padé approximation, where K_α is an integer in the α direction, to express the fluctuation and dissipation operators.[33] The HEOM in terms of Padé approximated frequency ν^α_k, where $k = \{0, 1, \cdots, K_\alpha\}$ with $\nu^\alpha_0 = \gamma_\alpha$, are then expressed as[25,27]

$$\frac{d}{dt} \hat{\rho}_{\{\mathbf{n}_\alpha\}} = -\left[\frac{i}{\hbar} \hat{H}^\times_S + \sum_{\alpha=x,y,z} \sum_{k=0}^{K_\alpha} (n^\alpha_k \nu^\alpha_k) \right] \hat{\rho}_{\{\mathbf{n}_\alpha\}}$$

$$- \frac{i}{\hbar} \sum_{\alpha=x,y,z} \sum_{k=0}^{K_\alpha} n^\alpha_k \hat{\Theta}^\alpha_k \hat{\rho}_{\{\mathbf{n}_\alpha - \mathbf{e}^k_\alpha\}}$$

$$- \frac{i}{\hbar} \sum_{\alpha=x,y,z} \sum_{k=0}^{K_\alpha} \hat{V}^\times_\alpha \hat{\rho}_{\{\mathbf{n}_\alpha + \mathbf{e}^k_\alpha\}}, \tag{5}$$

where $\{\mathbf{n}_\alpha\} \equiv (\mathbf{n}_x, \mathbf{n}_y, \mathbf{n}_z)$ is a set of integers $\mathbf{n}_\alpha = (n_0^\alpha, n_1^\alpha, n_2^\alpha, \cdots, n_{K_\alpha}^\alpha)$ to describe the hierarchy elements and $\{\mathbf{n}_\alpha \pm \mathbf{e}_\alpha^k\}$ with the index k, where $\mathbf{e}_\alpha^k$ is the kth unit vector in the α direction. We introduced the hyper operators $\hat{A}^\times \hat{B} \equiv \hat{A}\hat{B} - \hat{B}\hat{A}$ and $\hat{A}^\circ \hat{B} = \hat{A}\hat{B} + \hat{B}\hat{A}$. for any operator $\hat{A}$ and $\hat{B}$, and $\hat{\Theta}_k^\alpha$ is defined as

$$\hat{\Theta}_0^\alpha = \frac{\eta_\alpha \gamma_\alpha}{\beta} \left(1 + \sum_{k=1}^{K_\alpha} \frac{2\eta_k \gamma_\alpha^2}{\gamma_\alpha^2 - \nu_k^{\alpha^2}}\right) \hat{V}_\alpha^\times - \frac{\eta_\alpha \gamma_\alpha}{2} (\hat{H}_S^\times \hat{V}_\alpha)^\circ,$$
(6)

and

$$\Theta_{k \neq 0}^\alpha = -\frac{\eta_\alpha \gamma_\alpha^2}{\beta} \frac{2\eta_k \nu_k^\alpha}{\gamma_\alpha^2 - \nu_k^{\alpha^2}} \hat{V}_\alpha^\times,$$
(7)

where β, η_α and γ_α are inverse temperature, anisotropic coupling strength, and bath parameter. In Eq. (5), $\hat{\rho}_{\{\mathbf{n}_\alpha\}}$ are auxiliary operators with a hierarchical structure. The zeroth member of the hiracical elements $\hat{\rho}_{\{\mathbf{n}_\alpha = 0\}}$ represents original reduced density operator. As $(\mathbf{n}_x, \mathbf{n}_y, \mathbf{n}_z)$ can take all combinations of non-negative integers, HEOM should be closed by "terminator".[13]

$$\sum_{\alpha=x,y,z} \sum_{k=0}^{K_\alpha} (n_k^\alpha \nu_k^\alpha) \hat{\rho}_{\{\mathbf{n}_\alpha\}} = -\frac{i}{\hbar} \sum_{\alpha=x,y,z} \sum_{k=0}^{K_\alpha} n_k^\alpha \hat{\Theta}_k^\alpha \hat{\rho}_{\{\mathbf{n}_\alpha - \mathbf{e}_\alpha^k\}}$$
(8)

for $\sum_{\alpha=x,y,z} \sum_{k=0}^{K} (n_\alpha^k \nu_k) \gg \Delta\omega_{\max}$, where $\Delta\omega_{\max}$ is the largest transition frequency.

We now introduce spherical coordinates (r, θ, ϕ). We consider the system part of the S-B interactions in the linear coupling case $(\hat{V}_x, \hat{V}_y, \hat{V}_z) \equiv (\hat{x}, \hat{y}, \hat{z})$. We then have $\hat{V}_x = r\sin(\theta)\cos(\phi)$, $\hat{V}_y = r\sin(\theta)\sin(\phi)$, and $\hat{V}_z = r\cos(\phi)$. The eigenfunctions of the Coulomb potential system are expressed as the product of radial wavefunctions, $R_{nl}(r)$, and spherical harmonics, $Y_{lm}(\theta, \phi)$, as

$$\psi_{n,l,m}(r, \theta, \phi) = R_{nl}(r) Y_{lm}(\theta, \phi),$$
(9)

where n, l, and m are the principal, angular momentum, and magnetic quantum numbers, respectively. We describe the eigenvector for this set of numbers as $|\{\Gamma\}\rangle = |\{n, l, m\}\rangle$. Then the HEOM elements are expressed as $\hat{\rho}_{\{\mathbf{n}_\alpha\}}(\Gamma, \Gamma'; t)$. Any operators such as $\hat{H}_S$ and $\hat{V}_\alpha$ are expressed in terms of matrix elements as $H_S(\Gamma, \Gamma') = \langle\Gamma|\hat{H}_S|\Gamma'\rangle$ and $V_\alpha(\Gamma, \Gamma') = \langle\Gamma|\hat{V}_\alpha|\Gamma'\rangle$.

C. Linear absorption spectrum

We demonstrate our formalism by depicting linear absorption spectrum, defined as:[27]

$$I_{\alpha'\alpha}(\omega) = \text{Im}\left(\frac{i}{\hbar}\right) \int_0^\infty dt e^{i\omega_1 t_1} \text{Tr}\left\{\hat{\mu}_{\alpha'}\hat{\mathcal{G}}(t)\hat{\mu}_\alpha^\times \hat{\rho}_{\text{eq}}\right\},$$
(10)

where $\hat{\mu}_x = \mu_0 \sin(\theta)\cos(\phi)$, $\hat{\mu}_y = \mu_0 \sin(\theta)\sin(\phi)$, and $\hat{\mu}_z = \mu_0 \cos(\phi)$, are the dipole operators and $\hat{\mathcal{G}}(t)$ is

Green's function in the absence of a laser interaction, evaluated from Eqs. (5), and $\hat{\rho}_{\text{eq}}$ is the equilibrium density operator. Hereafter, we set $\mu_0 = 1.0$.

In the reduced equation of motion approach, the density matrix is replaced by a reduced one. In the HEOM case, $\hat{\rho}_{tot}^{eq}$ is replaced by the hierarchy member $\hat{\rho}_{\{\mathbf{n}_\alpha\}}^{eq}(t)$. The Liouvillian in $\hat{\mathcal{G}}(t)$ is replaced using Eqs. (5)-(8).

We evaluate Eqs. (10) in the following five steps.[14,15] (i) We first run the computational program to evaluate Eqs. (5)-(8) for sufficiently long times from the temporal initial conditions to obtain a true thermal equilibrium state, the full hierarchy members $\hat{\rho}_{\{\mathbf{n}_\alpha\}}^{eq}$ are then used to set the correlated initial thermal equilibrium state. (ii) The system is excited by the first interaction $\hat{\mu}^\times$ at $t = 0$. (iii) The evolution of the perturbed elements is then computed by running the program for the HEOM up to time t. (iv) Finally, the respose functions defined in Eq. (10) is calculated as the expectation value of $\hat{\mu}$. A fast Fourier transform yields the spectrum.

For reference, we also depict the absorption spectrum without the bath. From Fermi's golden rule, this is given by

$$I_{\alpha'\alpha}(\omega) = \sum_{mn} \mu_{\alpha'}^{mn} \mu_\alpha^{nm} \frac{e^{-\beta E_m} - e^{-\beta E_n}}{Z}$$
$$\times \delta\left(\hbar\omega + E_m - E_n\right)$$
(11)

where $Z = \sum_n e^{-\beta E_n}$ is the partition function and $\mu_\alpha^{mn} = \langle m|\hat{\mu}_\alpha|n\rangle$.

Throughout this paper, we use the basis given in Eq. (9) for the Columb potential system Eq. (2). Then the electronic transitions obey selection rules, allowing only transitions with angular momentum and magnetic quantum numbers $l = \pm 1$, $m = 0, \pm 1$. (see Table I). However, the peak positions in the absorption spectrum are determined solely by the difference in principal quantum numbers n. The transition frequency $\omega_{nn'}$ between state n to n' is given by the Rydberg formula:

$$\hbar\omega_{nn'} = R\left(\frac{1}{n^2} - \frac{1}{n'^2}\right)$$
(12)

Here, R denotes the Rydberg constant, and its value varies depending on the system under consideration in our simulations. In our simulations, we set $R = 1/2$.

III. NUMERICAL DEMONSTRATIONS: LINEAR ABSORPTION SPECTRUM

The Coulomb potential parameters are set to $A = 1$ and $M = 1$. The inverse noise correlation times are all fixed to $\gamma_x = \gamma_y = \gamma_z = 1$. We adopted 55 energy eigenstates, encompassing all eigenstates from principal quantum number $n = 1$ to $n = 5$. The number of hierarchical layers for each heat bath was set to $N_\alpha = 2$ using the Padé approximation of the [0/1] form.

We ran the AO-HEOM code using Python 3.13.5, along with CuPy 13.4.1 to enable CUDA support,

n' \ n	2	3	4	5	series
1	0.375	0.44444	0.46875	0.48	Lyman
2		0.06944	0.09375	0.105	Balmer
3			0.02430	0.03555	Paschen
4				0.01125	Brackett

TABLE I. Frequencies and series of absorption transitions from initial quantum state n to final states n' (up to $n' = 5$) in a Coulomb potential system evaluated from Eq. (12) with $R = 1/2$.
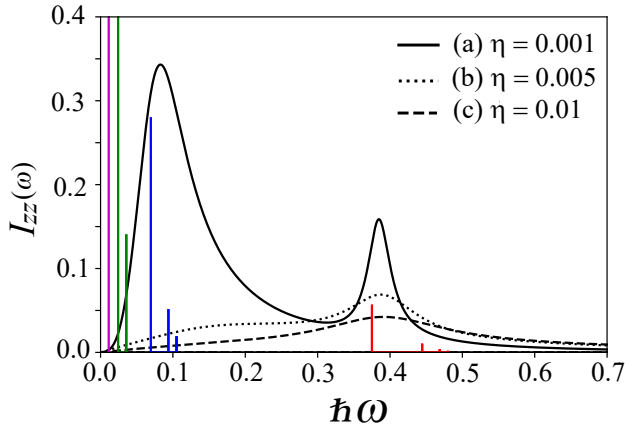

FIG. 1. Linear absorption spectra $I_{zz}(\omega)$ in the z direction for three different S–B coupling strengths: (a) weak (solid curve with $\eta = 0.001$), (b) intermediate (dotted curve with $\eta = 0.005$), and (b) strong (dashed curve with $\eta = 0.01$) at inverse temperature $\beta = 1.0$. To compare with the AO-HEOM results, we plotted the spectral peaks calculated from the golden rule [Eq. (11)] scaled by a factor of 0.2. Among these, the red lines correspond to the Lyman series, the blue lines to the Balmer series, the green lines to the Paschen series, and the pink lines to the Brackett series.

NumPy 2.2.5, and SciPy 1.15.3 for special functions and numerical integration. To solve the time-dependent HEOM equations, we used the fourth-order Runge–Kutta method. For computing the transition matrix, we applied SciPy's quad function, which is based on the FORTRAN QUADPACK library.

The computations were performed on a system equipped with an Intel Core i9-13900KF CPU and an NVIDIA GeForce RTX 4090 GPU, using CUDA Toolkit version 11.8. Each simulation with 3000 time steps required approximately 2.4 GB of GPU memory and 20,000 seconds of computation time.

We consider the isotropic bath case, where the coupling strengths are equal in all directions: $\eta_x = \eta_y = \eta_z = \eta$. The spectra in Fig. 1 were computed using Eq. (10) under fixed temperature conditions $\beta = 1.0$. To highlight the role of thermal fluctuations and dissipation in a Coulomb potential system, we intentionally consider an unphysically high-temperature bath with strong S–B coupling. For instance, in hydrogen, $\beta = 1.0$ corresponds to approximately 3×10^5K. Note that the value of R is typically an order of magnitude lower for color centers. For ionic liquids, where the potential includes shielding effects, the temperature scale is reduced by up to two orders of magnitude.

In the weak coupling regime (solid curve in Fig. 1), two distinct peaks are observed. According to Eq. (12) and the selection rules (see also Table I), the peak near $\hbar\omega = 0.08$ corresponds to the 2S→3P (Balmer-α) and 2S→4P (Balmer-β) transitions. Accordingly, the peak near $\hbar\omega = 0.4$ corresponds to the 1S→2P (Lyman-α) transition. Additional transitions such as 1S→3P (Lyman-β) and 1S→4P (Lyman-γ) should appear at higher frequencies, but they appear broadened and indistinct under these conditions. The Balmer transition peak is prominent because the population of the 2S state is well populated at this temperature.

According to the Golden Rule calculations, the AO-HEOM results are expected to show peaks from the Paschen and Brackett series at frequencies below $\omega = 0.5$. However, these long-period oscillations are suppressed by dissipation and therefore do not appear. To verify this, we repeated the calculation for $n' = 4$ and compared the results, but found no significant difference (See Appendix B).

In cases (b) and (c), where the coupling strength to the baths is increased, the two spectral peaks broaden and eventually merge, rendering them indistinguishable. This effect originates from S-B entanglement,[15] which suppresses the discrete spectral features characteristic of the Coulomb system. As the coupling strength increases, the contribution from the Balmer series is suppressed, similar to the Paschen and Brackett series, while the contribution from the Lyman series becomes greater. Such behavior lies beyond the scope of perturbative approaches and cannot be captured under the commonly employed factorization assumptions.

Figure 2 presents $I_{zz}(\omega)$ at (a) high ($\beta = 0.5$) and (b) low ($\beta = 1.5$) temperatures, with a fixed S-B coupling strength of $\eta = 0.001$. The result for the intermediate temperature ($\beta = 1.0$) is shown as the solid curve in Fig. 1.

As the temperature increases (i.e., as β decreases), spectral peaks exhibit noticeable broadening due to enhanced thermal fluctuations. Additionally, slight blue shifts in peak positions are observed in the high-frequency region, reflecting increased population of excited states at elevated temperatures.

At $\beta = 0.5$, the excited population of the 2S state increases, but the spectral peak corresponding to the Balmer−α transition is notably suppressed due to thermal relaxation, whereas the intensities of the Balmer-β and Balmer-γ peaks are enhanced. At lower tempera-
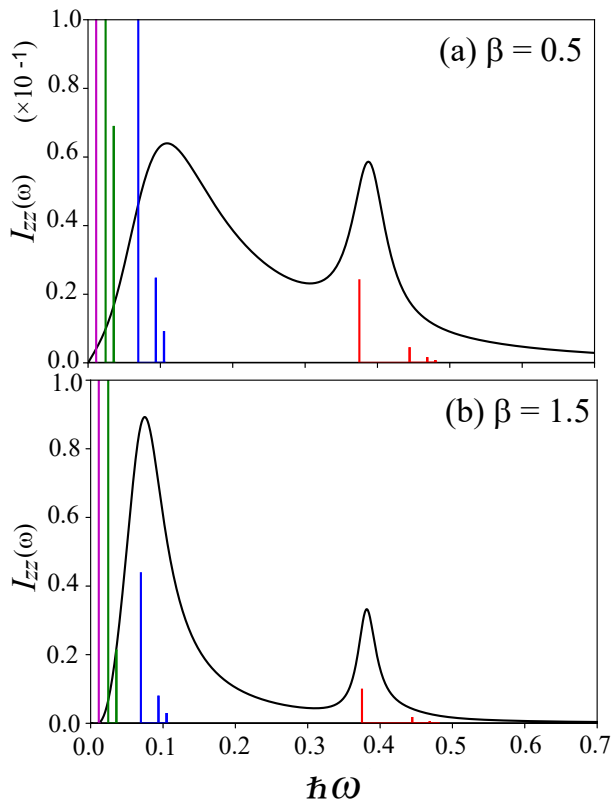
FIG. 2. Linear absorption spectra $I_{zz}(\omega)$ at (a) high ($\beta = 0.5$) and (b) low temperatures ($\beta = 0.5$) cases, with a fixed S-B coupling of $\eta = 0.001$. The result for the intermediate temperature ($\beta = 1.0$) is shown as the solid curve in Fig. 1. To compare with the AO-HEOM results, we plotted the spectral peaks calculated from the golden rule [Eq. (11)] scaled by a factor of 0.2. Among these, the red lines correspond to the Lyman series, the blue lines to the Balmer series, the green lines to the Paschen series, and the pink lines to the Brackett series.

tures, where thermal relaxation is less pronounced, the Balmer-α transition remains the dominant contributor to the emission spectrum.

IV. CONCLUSION

We rigorously investigated the quantum mechanical effects of thermal fluctuations and dissipation in a Coulomb potential system using a Hamiltonian that incorporates the 3D-RISB model. Due to the uncertainty principle relating energy fluctuations to correlation times, quantum thermal noise must be treated as a non-Markovian process. Accordingly, we adopted the

HEOM formalism, which provides a numerically "exact," non-perturbative, non-Markovian description of system dynamics.

To validate this approach, we computed linear absorption spectra across a range of temperatures and system-bath coupling strengths. Notably, we observed temperature- and coupling-dependent modifications in the spectral profiles of Lyman and Balmer transitions. We found that in the presence of fluctuation and dissipation, transitions from high principal quantum numbers -such as those observed in the Paschen and Brackett series- are largely suppressed due to their origin in long-period oscillations, and thus contribute negligibly. Although this study only investigated isotropic thermal environments, the HEOM framework can also address correlated thermal noise components from different directions.[27,32] . We also note that when employing the Caldeira—Leggett model with a bath lacking rotational symmetry, the results are classical behavior, with no discernible quantum transition features.[25,30] In contrast, the classical limit of our fully quantum framework yields results in agreement with the Caldeira—Leggett model and Langevin dynamics.

Our theory is based on a kinetic equation describing the energy exchange between the system and the environment through thermal fluctuations and dissipation. Our methodology is based on the HEOM formalism and can also calculate higher-order nonlinear spectra, such as two-dimensional spectrum.[14,15] Moreover, it is also possible to include gauge fields.[26] By extending this theory to molecules, we can study electron transfer and nonlinear spectra at finite temperatures directly using molecular orbital theory. We will continue such attempts in subsequent papers.

AUTHOR DECLARATIONS

Conflict of Interest

The authors have no conflicts to disclose.

DATA AVAILABILITY

The data that support the findings of this study are available from the corresponding author upon reasonable

request.

Appendix A: Basis function of Coulomb potential system

The eigenfunction of Hamiltonian Eq.(2) is expressed as a combination of associated Laguerre polynomials and spherical functions.

$$Y_l^m(\theta, \phi) = (-1)^{\frac{m+|m|}{2}} N_l^m e^{im\phi} P_l^{|m|}(\cos\theta) \qquad (A1)$$

with the normalization coefficient

$$N_l^m = \sqrt{\frac{2l+1}{4\pi} \frac{(l-m)!}{(l+m)!}} \qquad (A2)$$

and P_l^m are associated Legendre polynomials. However, we use the real form for numerical computation.

$$Y_{lm}(\theta, \phi) = \sqrt{2} N_l^m \sin(|m|\phi) P_l^{|m|}(\cos\theta), \quad m < 0 \quad (A3)$$

$$Y_{lm}(\theta, \phi) = \sqrt{2} N_l^m \cos(|m|\phi) P_l^{|m|}(\cos\theta). \quad m > 0 \quad (A4)$$

The radial part is

$$R_{nl}(r) = \sqrt{\left(\frac{2MA}{n}\right)^3 \frac{(n-l-1)!}{2n(n+l)!}}$$
$$e^{-MAr/n} \left(\frac{2MAr}{n}\right)^l L_{n-l-1}^{(2l+1)}\left(\frac{2MAr}{n}\right), \quad (A5)$$

where $L_{n-l-1}^{(2l+1)}$ are associated Laguerre polynomials.

Appendix B: Suppression of excited-state transitions by baths

In the high-temperature regime considered in this study, Fermi's golden rule]Eq. (11)] predicts that low-frequency excited states should contribute to the absorption spectrum (see vertical markers in Figs. 1 and 2). However, our results reveal that these contributions are effectively suppressed in the presence of thermal baths.

To illustrate this effect, we computed the absorption spectra for varying principal quantum numbers $n = 2$ to 5, corresponding to a total eigenstate count ranging from 5 to 55. The inverse temperature and S–B coupling strength were fixed at $\beta = 1.0$ and $\eta = 0.01$, respectively. All spectra were normalized to their maximum peak intensity for direct comparison.

As the basis set expands, the spectral profile converges, with negligible shifts in peak position. At this temperature, a substantial number of excited states above $n = 3$ are thermally populated, and several peaks predicted by the golden rule are expected to emerge. Nevertheless, the spectral shape in the corresponding frequency region exhibits minimal dependence on n. This insensitivity
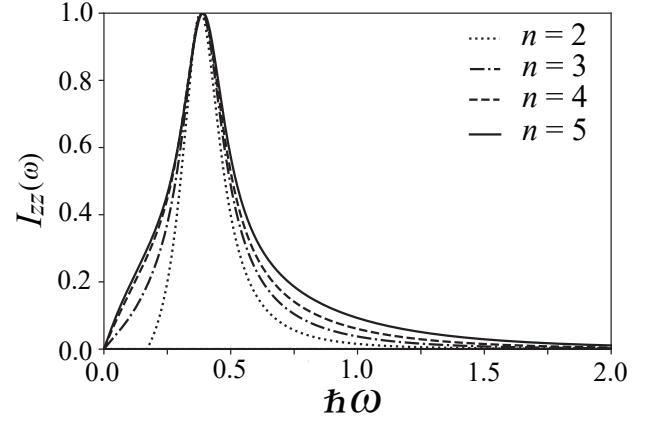

FIG. 3. Linear absorption spectra $I_{zz}(\omega)$ in the z direction for principal quantum numbers ranging from $n = 2$ to 5. The inverse temperature and the S-B coupling are fixed at $\beta = 1.0$ and $\eta = 0.01$. Each curve is normalized to its maximum peak intensity.

arises because the low-frequency peaks associated with long-period oscillations are quickly relaxed through interactions with the thermal environment.

These findings suggest that, in simulations incorporating thermal baths, it is not necessary to include a large number of excited states to accurately capture the spectral features.

[1] I. Tugov, On the Theory of Coulomb Interaction, NASA technical translation (National Aeronautics and Space Administration, 1967).

[2] H. Van Haeringen, Charged-particle interactions: theory and formulas (Coulomb Press, 1985).

[3] K. Seddon, Quill Handbook of Ionic Liquid (Quill, 2008) first published in 2008.

[4] W. Freyland, Coulombic Fluids: Bulk and Interfaces, Springer Series in Solid-State Sciences (Springer Berlin Heidelberg, 2011).

[5] M. Klein, Classical Planar Scattering by Coulombic Potentials, Lecture Notes in Physics Monographs, Vol. 13 (Springer, 2014) p. 147.

[6] D. G. Kanhere, A. Farazdel, and V. H. Smith, "Positron annihilation from f centers of alkali halide crystals," Phys. Rev. B **35**, 3131–3137 (1987).

[7] C. K. Ong, "Lattice static calculation of f-centre absorption energy in caesium halides," Journal of Physics C: Solid State Physics **15**, 427 (1982).

[8] T. Muto, "Theory of the f-centers of coloured alkali halide crystals. part i structure of f-absorption bands*," Progress of Theoretical Physics **4**, 181–192 (1949).

[9] A. A. Othman, M. de Montigny, and F. Marsiglio, "The coulomb potential in quantum mechanics revisited," American Journal of Physics **85**, 346–351 (2017), https://pubs.aip.org/aapt/ajp/article-pdf/85/5/346/13077589/346_1_online.pdf.

[10] M. O. Scully and W. E. Lamb, "Quantum theory of an optical maser. i. general theory," Phys. Rev. **159**, 208–226 (1967).

[11] B. Mollow and M. Miller, "The damped driven two-level atom," Annals of Physics **52**, 464–478 (1969).

[12] Y. Tanimura and R. Kubo, "Time evolution of a quantum system in contact with a nearly Gaussian-Markoffian noise bath," Journal of the Physical Society of Japan **58**, 101–114 (1989).

[13] A. Ishizaki and Y. Tanimura, "Quantum dynamics of system strongly coupled to low-temperature colored noise bath: Reduced

hierarchy equations approach," Journal of the Physical Society of Japan **74**, 3131–3134 (2005).

[14] Y. Tanimura, "Stochastic Liouville, Langevin, Fokker-Planck, and master equation qpproaches to quantum dissipative systems," Journal of the Physical Society of Japan **75**, 082001 (2006).

[15] Y. Tanimura, "Numerically "exact" approach to open quantum dynamics: The hierarchical equations of motion (HEOM)," The Journal of Chemical Physics **153**, 020901 (2020).

[16] A. J. Leggett, S. Chakravarty, A. T. Dorsey, M. P. A. Fisher, A. Garg, and W. Zwerger, "Dynamics of the dissipative two-state system," Rev. Mod. Phys. **59**, 1–85 (1987).

[17] R. Silbey and R. A. Harris, "Variational calculation of the dynamics of a two level system interacting with a bath," The Journal of Chemical Physics **80**, 2615–2617 (1984).

[18] C. Hsieh, J. Liu, C. Duan, and J. Cao, "A nonequilibrium variational polaron theory to study quantum heat transport," The Journal of Physical Chemistry C **123**, 17196–17204 (2019).

[19] S. Koyanagi and Y. Tanimura, "Thermodynamic quantum Fokker–Planck equations and their application to thermostatic Stirling engine," The Journal of Chemical Physics **161**, 112501 (2024), arXiv:2408.01083.

[20] S. Koyanagi and Y. Tanimura, "Hierarchical equations of motion for multiple baths (HEOM-MB) and their application to Carnot cycle," The Journal of Chemical Physics **161**, 162501 (2024), arXiv:2408.02249.

[21] N. Makri, "Numerical path integral techniques for long time dynamics of quantum dissipative systems," Journal of Mathematical Physics **36**, 2430–2457 (1995), https://pubs.aip.org/aip/jmp/article-pdf/36/5/2430/19149255/2430_1_online.pdf.

[22] N. Makri and D. E. Makarov, "Tensor propagator for iterative quantum time evolution of reduced density matrices. i. theory," The Journal of Chemical Physics **102**, 4600–4610 (1995), https://pubs.aip.org/aip/jcp/article-pdf/102/11/4600/19014630/4600_1_online.pdf.

[23] N. Makri and D. E. Makarov, "Tensor propagator for iterative quantum time evolution of reduced density matrices. ii. numerical methodology," The Journal of Chemical Physics **102**, 4611–4618 (1995), https://pubs.aip.org/aip/jcp/article-pdf/102/11/4611/19015655/4611_1_online.pdf.

[24] Y. Gefen, E. Ben-Jacob, and A. O. Caldeira, "Zener transitions in dissipative driven systems," Phys. Rev. B **36**, 2770–2782 (1987).

[25] Y. Iwamoto and Y. Tanimura, "Linear absorption spectrum of a quantum two-dimensional rotator calculated using a rotationally invariant system-bath hamiltonian," The Journal of Chemical Physics **149**, 084110 (2018).

[26] H. Yang, S. Koyanagi, and Y. Tanimura, "Quantum hierarchical fokker-planck equations of motion with gauge fields in u(1) symmetry: Application to aharonov-bohm ring in a dissipative environment," The Journal of Chemical Physics **16x**, xxxx (202x).

[27] Y. Iwamoto and Y. Tanimura, "Open quantum dynamics of a three-dimensional rotor calculated using a rotationally invariant system-bath Hamiltonian: Linear and two-dimensional rotational spectra," The Journal of Chemical Physics **151**, 044105 (2019).

[28] L. Chen, M. F. Gelin, and W. Domcke, "Orientational relaxation of a quantum linear rotor in a dissipative environment: Simulations with the hierarchical equations-of-motion method," The Journal of Chemical Physics **151**, 034101 (2019).

[29] Y. Tanimura, "Reduced hierarchical equations of motion in real and imaginary time: Correlated initial states and thermodynamic quantities," The Journal of Chemical Physics **141**, 044114 (2014).

[30] Y. Suzuki and Y. Tanimura, "Two-time correlation function of a two-dimensional quantal rotator in a colored noise," Journal of the Physical Society of Japan **71**, 2414–2426 (2002).

[31] Y. Tanimura and P. G. Wolynes, "Quantum and classical Fokker-Planck equations for a Gaussian-Markovian noise bath," Phys. Rev. A **43**, 4131–4142 (1991).

[32] H. Takahashi and Y. Tanimura, "Open quantum dynamics theory of spin relaxation: Application to μsr and low-field NMR spectroscopies," Journal of the Physical Society of Japan **89**, 064710 (2020).

[33] J. Hu, R.-X. Xu, and Y. Yan, "Communication: Padé spectrum decomposition of Fermi function and Bose function," The Journal of Chemical Physics **133**, 101106 (2010).